Percept-Aware Surgical Planning for Visual Cortical Prostheses with Vascular Avoidance

Galen Pogoncheff[1], Alvin Wang[1,2], Jacob Granley[1], and Michael Beyeler[1,3]

[1] Department of Computer Science, University of California, Santa Barbara
[2] School of Computer Science, Carnegie Mellon University
[3] Department of Psychological & Brain Sciences, University of California, Santa Barbara
mbeleyer@ucsb.edu

Abstract. Cortical visual prostheses aim to restore sight by electrically stimulating early visual cortex (V1). As high-density and flexible neural interfaces emerge, electrode placement within folded cortex becomes a critical surgical planning problem. Existing strategies emphasize visual-field coverage and anatomical heuristics, but do not directly optimize predicted perceptual outcomes under safety constraints. We present a percept-aware framework that formulates cortical electrode placement as constrained optimization in anatomical space. Electrode coordinates are treated as learnable parameters and optimized end-to-end using a differentiable model of prosthetic vision. The objective minimizes task-level perceptual error while incorporating vascular avoidance and gray matter feasibility. Using realistic folded cortical geometry (FreeSurfer *fsaverage*), we evaluate the method on simulated reading and natural-image tasks. Percept-aware optimization improves reconstruction fidelity relative to visual-field tiling and improves or matches coverage-based placement depending on task structure. Vascular constraints eliminate safety-margin violations with only modest effects on perceptual performance, and the framework supports co-optimization of multi-electrode thread configurations under fixed insertion budgets. These results show how differentiable percept models can support anatomically grounded, safety-aware planning for cortical visual prostheses.

Keywords: Visual Prostheses · Surgical Planning · Neural Interfaces

1 Introduction

Cortical visual neuroprostheses aim to restore sight by electrically stimulating early visual cortex, eliciting visual percepts known as phosphenes [10]. With the emergence of high-density and flexible neural interfaces [21, 20], surgeons face a critical planning question: where should electrodes be placed to maximize functional visual benefit?

Large-scale stimulation of primary visual cortex (V1) has demonstrated phosphene-based pattern vision in non-human primates [8], but translation to humans is complicated by cortical folding and inter-individual variability [2]. The functional organization of early visual cortex is nevertheless largely predictable from cortical anatomy [1], which is especially important in blind patients where visually driven fMRI mapping is often infeasible [24]. Electrode placement and cortical geometry therefore jointly shape the resulting phosphene map.

Current placement strategies rely on anatomical landmarks and retinotopic maps [11], targeting foveal representation while avoiding vasculature. Although safety-aware, these approaches remain geometric and coverage-driven rather than optimized for predicted perceptual fidelity. Prior work has optimized stimulation for fixed implants or arranged electrodes to maximize visual-field coverage [7, 17], but perceptual objectives and surgical constraints have not been jointly optimized within a unified planning framework.

Computational modeling has shown that stimulation parameters and electrode location shape phosphene structure [4, 15, 12]. These models suggest that placement should be evaluated not only by anatomical access or visual-field coverage, but also by the percepts expected from the resulting electrode map.

We introduce a model-driven approach for pre-operative planning that directly optimizes cortical electrode placement for perceptual fidelity under anatomical constraints. Electrode coordinates are treated as learnable parameters and optimized end-to-end using differentiable percept models. The framework incorporates retinotopic mapping and vascular avoidance, enabling percept-aware optimization on realistic folded cortex. We demonstrate the method on the FreeSurfer *fsaverage* cortical template, providing a consistent anatomical reference space for optimization.

The main contributions of our work include (1) a percept-aware optimization framework for three-dimensional cortical electrode placement that directly minimizes predicted task-relevant perceptual error, (2) explicit integration of vascular avoidance and anatomical feasibility constraints into the placement optimization, and (3) demonstration that optimized configurations can reduce cortical insertions while preserving functional performance.

2 Related Work

Visual neuroprosthesis optimization has largely followed two lines: optimizing stimulation for fixed implants and optimizing implant placement for visual-field coverage. Our work connects these lines by optimizing cortical electrode placement using a perceptual objective under anatomical constraints.

Prior work on fixed implants has optimized current amplitudes and electrode combinations [22, 6], calibrated electrode sensitivity profiles [13], and learned image-to-stimulation encoding strategies [14, 23]. These approaches improve predicted perceptual outcomes but assume fixed implant geometry and therefore do not address surgical placement.

A complementary line of work examines how implant location affects perceptual structure. In retinal implants, electrode position shapes phosphene geometry through axonal organization [4], motivating model-based selection of im-

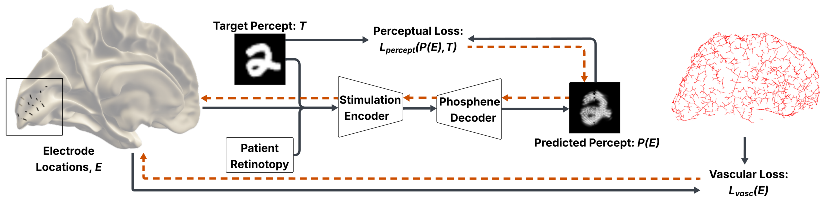

Fig. 1. Percept-aware optimization framework. Electrode coordinates on FreeSurfer *fsaverage* anatomy are mapped through retinotopy and a differentiable prosthetic vision model to predict elicited percepts, then updated to minimize perceptual error under vascular safety constraints. Solid arrows indicate forward simulation; dashed arrows indicate gradient-based coordinate updates.

plant configurations [3] and visual-field tiling strategies [7]. In cortex, retinotopic maps have been used to position electrodes to maximize projected visual-field coverage [17]. These methods optimize geometric coverage rather than task-level perceptual fidelity and generally do not integrate surgical constraints.

Literature Gap: Existing work either optimizes stimulation for fixed implants or optimizes placement using coverage-based objectives. Perceptual fidelity, task-relevant utility, and surgical constraints have not been jointly optimized within a planning framework. In contrast, we formulate cortical electrode placement as a percept-aware optimization problem in 3D brain space, integrating retinotopy and vascular constraints to support pre-operative surgical planning.

3 Methods

3.1 Surgical Planning Formulation

We formulate cortical electrode placement as a constrained optimization in three-dimensional anatomical space. Let $\Omega \subset \mathbb{R}^3$ denote the feasible gray matter region in early visual cortex. Electrode locations are parameterized as $E = \{\mathbf{p}_e\}_{e=1}^{N}$, where $\mathbf{p}_e = (x_e, y_e, z_e) \in \Omega$ represents the cortical coordinate of electrode e, and N is the fixed number of stimulation sites determined by device design.

Given a retinotopic map, a vascular map, and task-relevant target percepts $T \sim \mathcal{D}$, the goal is to optimize electrode locations for predicted perceptual fidelity while satisfying anatomical safety constraints (Fig. 1). A differentiable forward model maps electrode coordinates to predicted percepts, enabling gradient-based optimization directly in anatomical space.

We solve for optimal placement via the following multi-objective formulation: $E^* = \arg\min_{E \subset \Omega}\ \mathbb{E}_{T\sim\mathcal{D}}\left[\mathcal{L}_{\text{percept}}(P(E), T)\right] + \lambda_{\text{vasc}}\mathcal{L}_{\text{vasc}}(E) + \lambda_{\text{cortex}}\mathcal{L}_{\text{cortex}}(E)$, where $\mathcal{L}_{\text{percept}}$ measures task-level perceptual error, $\mathcal{L}_{\text{vasc}}$ penalizes vascular safety-margin violations, and $\mathcal{L}_{\text{cortex}}$ enforces anatomical feasibility.

3.2 Anatomical Representation

Electrode placement was performed on the FreeSurfer *fsaverage* cortical template. The template provides a folded gray matter surface mesh and volumetric representation, enabling optimization directly within realistic cortical geometry.

The feasible region Ω was defined as cortical gray matter within early visual cortex. Gray matter localization was obtained from the template segmentation and used to constrain electrode coordinates to anatomically plausible locations. Although laminar boundaries were not explicitly modeled, confinement to gray matter serves as a proxy for targeting layer 4, the typical stimulation depth for intracortical visual prostheses.

Retinotopic mappings were obtained from the Benson et al. [1] Bayesian retinotopy prior defined in *fsaverage* surface space. The cerebrovascular atlas [18] was registered to the same coordinate system, enabling direct computation of electrode-to-vessel distances. All anatomical constraints and percept simulations were therefore evaluated in a common neuroanatomical reference frame.

3.3 Perceptual Forward Model

We define a differentiable forward model that maps cortical electrode coordinates to predicted visual percepts. The model consists of two stages: (i) a retinotopic mapping from cortical space to visual field coordinates, and (ii) a phosphene generation model that predicts the elicited percept.

Retinotopic Mapping: For an electrode at cortical location $\mathbf{p}_e$, its visual field coordinate $\mathbf{s}_e$ is estimated by distance-weighted interpolation over the k nearest retinotopic sites, $\mathcal{N}_k(\mathbf{p}_e)$, each with cortical coordinate $\mathbf{c}_j$ and mapped visual field location $\mathbf{v}_j$:

$$\mathbf{s}_e = \frac{\sum_{j\in\mathcal{N}_k(\mathbf{p}_e)} w_{ej}\mathbf{v}_j}{\sum_{j\in\mathcal{N}_k(\mathbf{p}_e)} w_{ej}}, \quad w_{ej} = \frac{1}{\|\mathbf{p}_e - \mathbf{c}_j\|_2}. \tag{1}$$

Phosphene Generation: Stimulation amplitude a_e is sampled from the target at $\mathbf{s}_e$, and the percept is modeled as a sum of isotropic Gaussians with spread ρ: $P(x,y) = \sum_{e=1}^{N} a_e \exp\Big(-\frac{(x-\mathbf{s}_{e,x})^2+(y-\mathbf{s}_{e,y})^2}{2\rho^2}\Big)$.

This formulation provides a differentiable mapping from cortical electrode coordinates to image-space percepts, enabling gradient-based optimization in anatomical space. While Gaussian phosphenes with linear superposition provide a tractable approximation consistent with prior modeling work [11, 15], the framework readily generalizes to alternative, differentiable percept models.

Perceptual Objective: Perceptual fidelity is measured using a foveally weighted mean squared error: $\mathcal{L}_{\text{percept}}(P,T) = \sum_{(x,y)} w(x,y)\,(P(x,y) - T(x,y))^2$, where $w(x,y)$ increases toward the fovea to reflect the higher functional importance of central vision in many tasks.

3.4 Anatomical and Safety Constraints

Electrode placement is subject to anatomical feasibility and vascular safety constraints. These are incorporated as differentiable penalty terms within the optimization objective.

Avoidance of cortical vasculature is a primary safety consideration in intracortical implantation. Prior studies report vascular disruption extending up to 300 µm from insertion sites [5], motivating an explicit safety margin. Let $\mathcal{V}$ denote the vasculature and $d(\mathbf{p}_e, \mathcal{V})$ the nearest vessel distance. Vascular avoidance was penalized as

$$\mathcal{L}_{\text{vasc}}(E) = \frac{1}{|E|} \sum_{e \in E} \left[\max\left(0, \tau - d(\mathbf{p}_e, \mathcal{V})\right)\right]^2, \tag{2}$$

with safety margin $\tau = 300\,\mu\text{m}$.

Intracortical stimulation targets neurons within cortical gray matter. To ensure anatomically plausible placements, we penalize electrode coordinates outside the gray matter mask. Let $d_{\text{gm}}(\mathbf{p}_e)$ denote the signed distance to gray matter. We define $\mathcal{L}_{\text{cortex}}(E) = \frac{1}{|E|}\sum_{e \in E} d_{\text{gm}}(\mathbf{p}_e)^2$.

Together, these terms embed surgical feasibility directly into the differentiable planning framework, enabling trade-offs between functional performance and safety to be explored continuously during optimization.

3.5 Optimization Procedure

Optimization was performed using gradient-based updates in anatomical space. Because the forward percept model and constraint terms are differentiable w.r.t. electrode coordinates, gradients were computed via automatic differentiation. During optimization, vascular and gray matter penalties were jointly applied with perceptual loss, allowing electrode locations to be continuously adjusted to balance functional performance and surgical safety.

Electrode coordinates were initialized uniformly within the feasible cortical region Ω. We used the Adam optimizer with fixed learning rate and optimized electrode positions until convergence of the objective on training data. Experiments were performed in Python using TensorFlow. Optimization for a single configuration required less than 10 min. on a NVIDIA RTX 3090 GPU.

3.6 Experimental Protocol

Datasets: We evaluated placement strategies using two image datasets representing distinct functional goals of visual prostheses: handwritten digits from MNIST [9], approximating structured symbol recognition (e.g., reading), and natural images from CIFAR-10 [19], representing more complex visual scenes.

Experimental Configurations: Experiments were conducted across electrode counts, $N \in \{64 - 1024\}$, and phosphene spreads, $\rho \in \{500 - 1500\}$ µm. For each configuration, optimization was performed over 3 random initializations. For device-architecture experiments, we also considered threaded arrays inspired by flexible multi-electrode shanks [21], where multiple stimulation contacts share a common cortical insertion trajectory. These experiments fixed the number of cortical insertions at $N_{\text{insert}} = 128$ and optimized both entry location and trajectory.

Baselines: We compared the proposed percept-aware optimization against two placement strategies: (i) *Visual Field Tiling*, which uniformly tiles the visual field, and (ii) *Visual Field Coverage*, which optimizes electrode positions to maximize coverage of the visual field represented in the training images [17].

Evaluation Metrics: Perceptual fidelity was quantified using structural similarity index measure (SSIM) and mean squared error (MSE) between target images and simulated percepts, along with downstream classification accuracy. Learned perceptual metrics were not used because prosthetic percepts deviate from natural-image statistics, particularly at low electrode counts [14]. Classification accuracy was used only as a task proxy: we trained ResNet-50 classifiers [16] on target images and evaluated whether simulated phosphenes preserved information needed for symbol and object identification [13].

Statistical Analysis: Results were aggregated across experimental configurations and random initializations. Statistical comparisons between methods were performed using Wilcoxon signed-rank tests with significance threshold $p \leq 0.01$.

4 Results

4.1 Percept-Aware Optimization Improves Functional Fidelity

We first evaluated placement optimization without anatomical constraints to isolate functional performance. Across electrode counts and phosphene spread parameters, percept-aware optimization consistently reduced reconstruction error relative to both Visual Field Tiling and Visual Field Coverage.

On MNIST, percept-aware optimization reduced median MSE by up to 67.7% relative to tiling and 33.4% relative to coverage, increased downstream classification accuracy by 62.6% and 22.4%, respectively, and yielded corresponding improvements in SSIM (Table 1). On CIFAR-10, percept-aware placement substantially outperformed tiling and achieved performance comparable to coverage-based optimization. The latter is expected because CIFAR-10 images typically

Table 1. Relative change in MSE, SSIM, and downstream classification accuracy (Acc.) of the proposed method versus baselines. Values are median percent difference [IQR] across electrode counts and phosphene spreads (ρ). * indicates $p \leq 0.01$.

Baseline	Dataset	Δ MSE (%) ↓	Δ SSIM (%) ↑	Δ Acc. (%) ↑
VF Tiling	MNIST	-67.7* [-73.6, -47.2]	11.1* [7.8, 16.7]	62.6* [28.9, 119.9]
VF Coverage		-33.4* [-42.0, -16.3]	4.7* [3.1, 7.3]	22.4* [7.8, 34.7]
VF Tiling	CIFAR-10	-58.4* [-87.4, -24.1]	57.4* [35.3, 102.2]	10.2* [5.5, 29.2]
VF Coverage		16.0 [-25.2, 39.1]	-10.6 [-24.7, 0.2]	-2.2 [-9.1, 6.25]

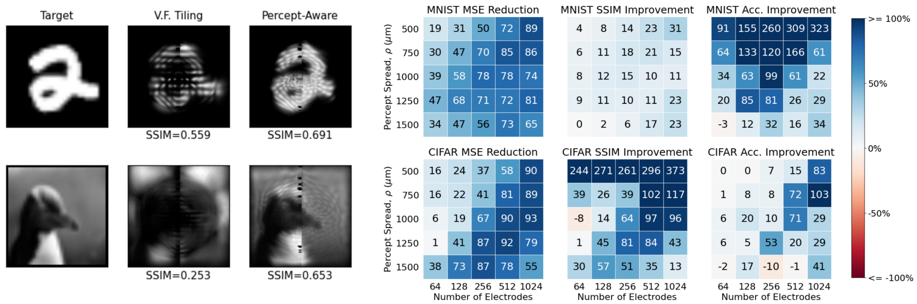

Fig. 2. Comparing percept-aware electrode optimization and Visual Field Tiling. *Left*: Simulated phosphenes for reading (MNIST) and natural image (CIFAR-10) tasks. *Right*: Relative changes in perceptual fidelity across experimental configurations; lower MSE and higher SSIM indicate better reconstruction.

occupy the full visual field, aligning coverage objectives with reconstruction fidelity. Qualitative examples (Fig. 2) show clearer symbol structure and improved spatial coherence under percept-aware placement.

4.2 Safety-Aware Optimization Preserves Perceptual Performance

We next incorporated vascular avoidance into the optimization objective. Without safety constraints, a large fraction of electrodes violated the 300 μm safety margin. Incorporating the vascular penalty eliminated all margin violations.

Perceptual quality changed only modestly in these simulations. Across configurations, SSIM decreased by only 1.7% on MNIST and 4.4% on CIFAR-10 relative to unconstrained optimization (Fig. 3), suggesting that functional performance can be largely maintained while satisfying clinically-motivated vascular safety constraints.

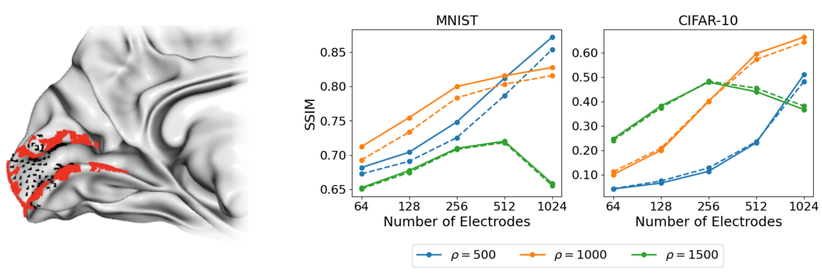

Fig. 3. Safety-aware electrode optimization with vascular constraints. *Left*: Cortical surface (*fsaverage* left occipital) with high-resolution vascular map (red, displayed in V1 only) and optimized electrode locations (black). *Right*: Percept SSIM scores without (solid lines) and with (dashed lines) vascular avoidance.

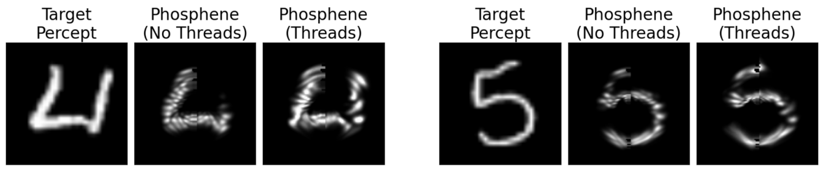

Fig. 4. Simulated phosphenes using percept-aware optimization with and without multi-electrode threads under a fixed number of cortical insertions (128). Threaded designs improve percept quality without increasing number of cortical insertions.

4.3 Device Architecture Co-Optimization with Threaded Arrays

We extended the framework to optimize threaded arrays, where multiple electrode contacts share a single cortical insertion trajectory. Under the fixed insertion budget defined above, threaded configurations improved perceptual fidelity relative to single-electrode placements (Fig. 4).

5 Discussion

We present a percept-aware surgical planning framework for cortical visual prostheses that directly optimizes electrode placement in three-dimensional brain space under anatomical constraints. By integrating differentiable percept modeling with realistic cortical geometry and vascular avoidance, the proposed approach aligns surgical decision-making with predicted functional outcomes.

Across simulated reading and natural image tasks, percept-aware placement improved reconstruction fidelity relative to visual-field tiling and provided task-dependent benefits relative to coverage-based strategies. Improvements were strongest for symbol-like images, whereas performance on CIFAR-10 was comparable to coverage-based placement, likely because natural images occupied much of the visual field and therefore aligned well with the coverage objective.

Several limitations remain. First, experiments were conducted on the widely used *fsaverage* template rather than subject-specific anatomy. However, the framework is fully compatible with patient-specific cortical reconstructions, retinotopic mapping (e.g., fMRI), and angiographic data. Second, the perceptual forward model uses simplified Gaussian phosphenes and linear superposition. Future work will incorporate more detailed biophysical models.Third, the present study evaluates the planning objective rather than a complete surgical workflow. In practice, optimized coordinates would need to be transformed into patient-specific stereotactic space and integrated with neuronavigation, trajectory planning, and intraoperative constraints. Thus, the current framework should be viewed as a pre-operative decision-support tool for comparing candidate implant configurations, not as a stand-alone intraoperative guidance system.

Overall, this work introduces perceptual objectives into computer-assisted planning for cortical neural interfaces and establishes a framework for anatomically grounded, safety-aware optimization of next-generation visual prostheses.

Disclosure of Interests

The authors declare no competing interests.

Acknowledgments

Supported by the National Library of Medicine of the National Institutes of Health (NIH) under Award Number DP2-LM014268. The content is solely the responsibility of the authors and does not necessarily represent the official views of the NIH.

References

1. Benson, N.C., Winawer, J.: Bayesian analysis of retinotopic maps. elife **7**, e40224 (2018)
2. Benson, N.C., Yoon, J.M.D., Forenzo, D., Engel, S.A., Kay, K.N., Winawer, J.: Variability of the Surface Area of the V1, V2, and V3 Maps in a Large Sample of Human Observers. Journal of Neuroscience **42**(46), 8629–8646 (Nov 2022). https://doi.org/10.1523/JNEUROSCI.0690-21.2022
3. Beyeler, M., Boynton, G.M., Fine, I., Rokem, A.: Model-Based Recommendations for Optimal Surgical Placement of Epiretinal Implants. In: Shen, D., Liu, T., Peters, T.M., Staib, L.H., Essert, C., Zhou, S., Yap, P.T., Khan, A. (eds.) Medical Image Computing and Computer Assisted Intervention – MICCAI 2019. pp. 394–402. Lecture Notes in Computer Science, Springer International Publishing (2019)
4. Beyeler, M., Nanduri, D., Weiland, J.D., Rokem, A., Boynton, G.M., Fine, I.: A model of ganglion axon pathways accounts for percepts elicited by retinal implants. Scientific Reports **9**(1), 1–16 (Jun 2019). https://doi.org/10.1038/s41598-019-45416-4
5. Bjornsson, C., Oh, S.J., Al-Kofahi, Y., Lim, Y., Smith, K., Turner, J., De, S., Roysam, B., Shain, W., Kim, S.J.: Effects of insertion conditions on tissue strain and vascular damage during neuroprosthetic device insertion. Journal of neural engineering **3**(3), 196 (2006)
6. Bratu, E., Dwyer, R., Noble, J.: A Graph-Based Method for Optimal Active Electrode Selection in Cochlear Implants. In: Martel, A.L., Abolmaesumi, P., Stoyanov, D., Mateus, D., Zuluaga, M.A., Zhou, S.K., Racoceanu, D., Joskowicz, L. (eds.) Medical Image Computing and Computer Assisted Intervention – MICCAI 2020. pp. 34–43. Lecture Notes in Computer Science, Springer International Publishing, Cham (2020). https://doi.org/10.1007/978-3-030-59716-0_4
7. Bruce, A., Beyeler, M.: Greedy Optimization of Electrode Arrangement for Epiretinal Prostheses. In: Medical Image Computing and Computer Assisted Intervention – MICCAI 2022. Springer International Publishing (2022). https://doi.org/10.1007/978-3-031-16449-1_57
8. Chen, X., Wang, F., Fernandez, E., Roelfsema, P.R.: Shape perception via a high-channel-count neuroprosthesis in monkey visual cortex. Science **370**(6521), 1191–1196 (Dec 2020). https://doi.org/10.1126/science.abd7435
9. Deng, L.: The mnist database of handwritten digit images for machine learning research [best of the web]. IEEE signal processing magazine **29**(6), 141–142 (2012)

10. Fernandez, E.: Development of visual Neuroprostheses: trends and challenges. Bioelectronic Medicine **4**(1), 12 (Aug 2018). https://doi.org/10.1186/s42234-018-0013-8
11. Fernández, E., Alfaro, A., Soto-Sánchez, C., Gonzalez-Lopez, P., Lozano, A.M., Peña, S., Grima, M.D., Rodil, A., Gómez, B., Chen, X., et al.: Visual percepts evoked with an intracortical 96-channel microelectrode array inserted in human occipital cortex. The Journal of clinical investigation **131**(23) (2021)
12. Fine, I., Boynton, G.M.: A virtual patient simulation modeling the neural and perceptual effects of human visual cortical stimulation, from pulse trains to percepts. Scientific Reports **14**(1), 17400 (Jul 2024). https://doi.org/10.1038/s41598-024-65337-1
13. Granley, J., Fauvel, T., Chalk, M., Beyeler, M.: Human-in-the-Loop Optimization for Deep Stimulus Encoding in Visual Prostheses. Thirty-seventh Conference on Neural Information Processing Systems (Nov 2023)
14. Granley, J., Relic, L., Beyeler, M.: Hybrid Neural Autoencoders for Stimulus Encoding in Visual and Other Sensory Neuroprostheses. In: Advances in Neural Information Processing Systems. vol. 35, pp. 22671–22685 (Dec 2022)
15. van der Grinten, M.L., de Ruyter van Steveninck, J., Lozano, A., Pijnacker, L., Rueckauer, B., Roelfsema, P., Gerven, M.v., Wezel, R.v., Guclu, U., Gucluturk, Y.: Towards biologically plausible phosphene simulation for the differentiable optimization of visual cortical prostheses (Dec 2024). https://doi.org/10.7554/eLife.85812
16. He, K., Zhang, X., Ren, S., Sun, J.: Deep residual learning for image recognition. In: Proceedings of the IEEE conference on computer vision and pattern recognition. pp. 770–778 (2016)
17. van Hoof, R., Lozano, A., Wang, F., Klink, P.C., Roelfsema, P.R., Goebel, R.: Optimal placement of high-channel visual prostheses in human retinotopic visual cortex (2025). https://doi.org/10.1088/1741-2552/adaeef
18. Ii, S., Kitade, H., Ishida, S., Imai, Y., Watanabe, Y., Wada, S.: Multiscale modeling of human cerebrovasculature: A hybrid approach using image-based geometry and a mathematical algorithm. PLoS computational biology **16**(6), e1007943 (2020)
19. Krizhevsky, A., Hinton, G., et al.: Learning multiple layers of features from tiny images (2009)
20. Merken, L., Schelles, M., Ceyssens, F., Kraft, M., Janssen, P.: Thin flexible arrays for long-term multi-electrode recordings in macaque primary visual cortex. Journal of Neural Engineering **19**(6), 066039 (Dec 2022). https://doi.org/10.1088/1741-2552/ac98e2
21. Musk, E., Neuralink: An Integrated Brain-Machine Interface Platform With Thousands of Channels. Journal of Medical Internet Research **21**(10), e16194 (Oct 2019). https://doi.org/10.2196/16194
22. Shah, N.P., Madugula, S., Grosberg, L., Mena, G., Tandon, P., Hottowy, P., Sher, A., Litke, A., Mitra, S., Chichilnisky, E.: Optimization of Electrical Stimulation for a High-Fidelity Artificial Retina. In: 2019 9th International IEEE/EMBS Conference on Neural Engineering (NER). pp. 714–718 (Mar 2019). https://doi.org/10.1109/NER.2019.8716987
23. de Ruyter van Steveninck, J., Güçlü, U., van Wezel, R., van Gerven, M.: End-to-end optimization of prosthetic vision. Journal of Vision **22**(2), 20 (Feb 2022). https://doi.org/10.1167/jov.22.2.20
24. Striem-Amit, E., Ovadia-Caro, S., Caramazza, A., Margulies, D.S., Villringer, A., Amedi, A.: Functional connectivity of visual cortex in the blind follows retinotopic organization principles. Brain: A Journal of Neurology **138**(Pt 6), 1679–1695 (Jun 2015). https://doi.org/10.1093/brain/awv083